Remote Sensing Letters

ISSN: 2150-704X (Print) 2150-7058 (Online) Journal homepage: www.tandfonline.com/journals/trsl20

River network based characterization of errors in remotely sensed rainfall products in hydrological applications

Mohamed ElSaadani, Witold F. Krajewski & Dale L. Zimmerman

To cite this article: Mohamed ElSaadani, Witold F. Krajewski & Dale L. Zimmerman (2018) River network based characterization of errors in remotely sensed rainfall products in hydrological applications, Remote Sensing Letters, 9:8, 743-752, DOI: 10.1080/2150704X.2018.1475768

To link to this article: https://doi.org/10.1080/2150704X.2018.1475768

Published online: 24 May 2018.

REMOTE SENSING LETTERS
2018, VOL. 9, NO. 8, 743–752
https://doi.org/10.1080/2150704X.2018.1475768

Taylor & Francis
Taylor & Francis Group

River network based characterization of errors in remotely sensed rainfall products in hydrological applications

Mohamed ElSaadani [a], Witold F. Krajewski [a] and Dale L. Zimmerman [b]

[a]IIHR—Hydroscience & Engineering, The University of Iowa, Iowa City, IA, USA; [b]Department of Statistics and Actuarial Science, The University of Iowa, Iowa City, IA, USA

ABSTRACT

The authors propose a hydrologic evaluation framework for gridded rainfall products. This framework makes use of the Spatial Stream Network (SSN) statistical method to provide spatial characterization of the discrepancies between two gridded rainfall products. The SSN method relies on using stream network length rather than the traditionally used Euclidean distances.It also accounts for the flow connectivity information between the network segments. This concept is relevant in hydrological modeling since rivers transport accumulated precipitation that occurred over different parts of the basins, and stream networks do not represent Euclidean space. To demonstrate, we used this framework to compare the satellite rainfall product called Integrated Multi-satellitE Retrievals for GPM (IMERG) with the ground-based Multi-Radar/Multi-Sensor (MRMS) rainfall product. The results show that the magnitudes of the rainfall discrepancies tend to decrease as rainfall accumulates in the downstream direction. However, the covariance range between these discrepancies is much larger along flow-connected stream network segments than in flow-unconnected stream segments. This in turn could have an effect on the error correlation of the predicted discharges. In addition, the spatial linear models of rainfall errors improved significantly with SSN based models in comparison to pure Euclidean separation distance models.

ARTICLE HISTORY
Received 3 July 2017
Accepted 3 May 2018

1. Introduction

Many studies have aimed to evaluate or enhance the performance of satellite rainfall products in hydrologic applications (e.g., Gourley et al. 2011; Vergara et al. 2014; Habib et al. 2014). A few studies have modeled the spatial dependence of the rainfall errors from different sensors but limited the considerations to the Euclidean space (e.g., Vergara et al. 2014; Mandapaka et al. 2009). This Euclidian based characterization is suitable for many applications such as runoff generation, evapotranspiration (ET), or soil moisture content estimation since these variables are continuous in Euclidean space. However, variables such as stream discharge are confined by the stream network, which is dichotomous in nature and a fractal (e.g., Rodriguez-Iturbe and Rinaldo 1997).

CONTACT Mohamed ElSaadani mohamedali-elsaadani@uiowa.edu IIHR—Hydroscience & Engineering, The University of Iowa, Iowa City, IA 52242

In this paper, we present an example of river network based characterization of uncertainties in remote sensing rainfall products. River networks act as low pass filters on highly variable rainfall and its estimates, but their averaging properties are different from those of Euclidean domains. Our application is limited to rainfall only but similar considerations, with substantially more difficulties, apply to the transformed variables of runoff and streamflow and their characteristics such as peak and low flows. We characterize spatial dependence of rainfall errors using the tools of geostatistics, namely the semi-variogram (e.g., Cressie 1993). In addition, we compare the performance of multiple spatial statistical linear models that utilize Euclidean or stream distance based covariance.

The stream network method we use to characterize the errors is described by Ver Hoef, Peterson, and Theobald (2006) and called the Spatial Stream Network (SSN). SSN accounts for the nested nature of the stream network by using stream distances and site connectivity information. Studies such as Ver Hoef, Peterson, and Theobald (2006), Ver Hoef and Peterson (2010), and Zimmerman and Ver Hoef (2017) proved that this method is substantially more accurate in modeling stream network variables such as water chemistry and temperature since it takes into account the transport of water from one location to another; they also discussed the various SSN covariance model types in details. Nevertheless, the SSN method has received little to no attention in hydrologic modeling studies but we find it highly relevant for applications since river networks play a dominant role.

2. Rainfall products and study area

In this study, we characterize spatial uncertainties of the satellite rainfall product Integrated MultisatellitE Retrievals for GPM (IMERG) Final Run (Huffman et al. 2015). IMERG combines rainfall estimates from Microwave (MW) sensors on board the Global Precipitation Measurement's (GPM) satellite constellation as well as estimates from Infrared (IR) sensors on board geostationary satellites (Hou et al. 2014). The IMERG product undergoes bias correction using the monthly rain gauge estimates provided by the Global Precipitation Climatology Centre (GPCC). The product has a half-hourly temporal resolution and is available on a 0.1° square grid with a global coverage between 60° N and 60 S° (Liu 2016). Our benchmark (reference) product in this study is the Multi-Radar Multi-Sensor (MRMS) Quantitative Precipitation Estimate (QPE). This product uses data from the Weather Surveillance Radar-1988 (WSR-88D) and is corrected using rain gauge data provided by the Hydrometeorological Automated Data System (HADS) (Zhang et al. 2013). The product is available on a 0.01° square grid and at hourly temporal resolution.

Our study area is a mid-sized Cedar River basin in eastern Iowa, USA with an overall drainage area of approximately 17,000 km^2. The shape of the basin and the width function of the river network are illustrated in Figure 1(a,b). The width function could be interpreted as a distribution of distances from the outlet. From Figure 1(b) it is evident that the majority of the pathways to the outlet have length between 150 and 300 km. The basin experienced a heavy rainfall event in September 2016, which resulted in the second highest river water level in history on 27 September 2016 (https://www.weather.gov/dvn/summary_09272016). We use this event as our test case for the evaluation. We use the digitized stream network provided by the National Hydrography Dataset Plus Version 2 (NHDPlus V2, http://www.horizon-systems.com/nhdplus/documentation.php) to obtain the necessary stream network

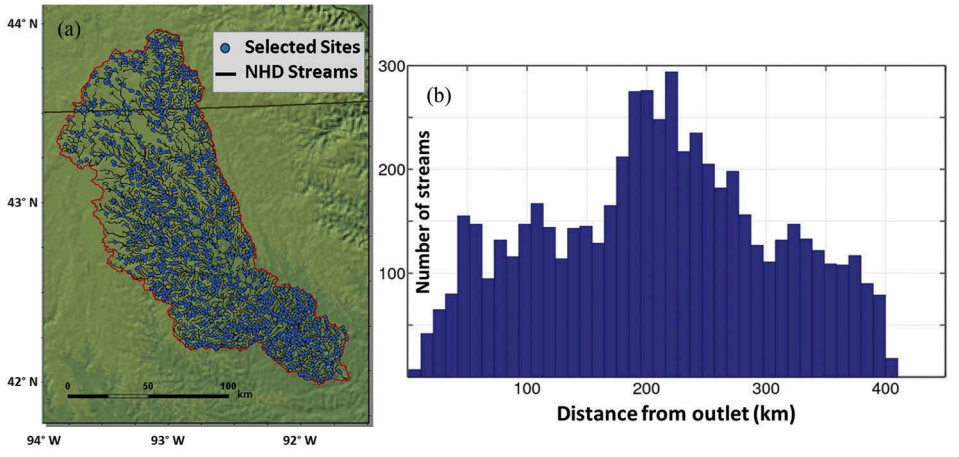

Figure 1. (*a*) The Cedar River basin located in eastern Iowa. The black lines represent the NHDPlus V2 stream network definition (Flowlines), while the blue points represents the sample sites located near the confluences of the network. (*b*) The width function of the basin showing the number of streams (*y*-axis) at different distances in km (*x*-axis) from the outlet.

information (e.g., stream distance, and stream served area). Other necessary information (e.g., connectivity, upstream distance from the basin outlet, and covariance function weights) is obtained using the Spatial Tools for the Analysis of River Systems (STARS) and SSN software packages described in Peterson and Ver Hoef (2014).

3. Methods

A good tool to estimate and visualize spatial dependence is the semi-variance which can be illustrated using the semi-variograms. Traditionally, the semi-variogram is constructed using Euclidean distance between the observation sites. However, for our stream network application, it is better to characterize the semi-variance in terms of stream distance rather than Euclidean distance. In addition, because some variables are impacted by the flow connectivity structure of the stream network (e.g., there is no water transport between unconnected locations as well as in the upstream direction), it is important to separate the measured distances into two categories. First, distances between flow-connected sites (e.g., the water flows directly from the upstream site location to the downstream site location) are equal to the length of the stream segments connecting the two sites. Second, distances between flow-unconnected sites are equal to the sum of the lengths of the two stream segments that connect each site to the nearest downstream connecting junction. Because of this distance categorization, we obtain two semi-variograms that when plotted simultaneously are called the Torgegram (Zimmerman and Ver Hoef 2017). If the spatial dependence of the variable of interest is not impacted by network connectivity, the flow-connected and flow-unconnected portions of the Torgegram should be similar; otherwise, they could be quite different.

The SSN covariance models used in prediction are based on Moving Average (MA) constructions (Ver Hoef, Peterson, and Theobald 2006). The derivation of the models is beyond the scope of this article. However, we briefly summarize how the models are obtained. The MA construction is created by considering a random variable to be equal to the integral of a MA function over a white noise process on the stream network. The MA function is only non-zero in one direction, either upstream or downstream. The value of the moving average function is largest at the observation site and decreases as it moves away from the site location. The smaller the separation distance between two sites, the greater the extent of overlap of those portions of the MA functions that are relatively large. This in turn will result in higher covariance.

Covariance models for which the corresponding MA function is only positive in the upstream direction are called tail-up models and they only allow flow-connected sites to be correlated. In this case, the MA function needs to split at upstream junctions with weights relative to the served areas of the streams intersecting at this junction. Since there is no overlap between the MA functions of flow-unconnected sites, their covariance is equal to zero. On the other hand, tail-down models have MA functions pointing downstream. Although useful for considering covariance between flow-unconnected sites; tail-down models assign the same, or an even larger, covariance value between flow-unconnected sites as they do between flow-connected sites with equivalent separation distance. This is not appropriate for many hydrologic variables since observations at flow-connected sites are usually more correlated than those at flow-unconnected sites that are separated by equivalent distances. Thus, as described in Ver Hoef, Peterson, and Theobald (2006), it is useful to construct a mixed spatial linear model that incorporates the covariance generated by a linear combination of some or all models (e.g., tail-up, tail-down, and Euclidean).

We follow the approach described in Quintero et al. (2016) and Cunha et al. (2015) in order to calculate the differences between the rainfall products in a stream network setting. We convert gridded rainfall products to a more hydrologically relevant representation by accumulating the rainfall for all size basins. Normalized by the drainage area, rainfall is assigned to the river network link that drains that area. We then subtract the evaluated product from the corresponding reference product thus obtaining a river network representation of the rainfall differences (errors). Strictly speaking, the reference product is also subject to estimation uncertainty (e.g., Villarini and Krajewski 2007) but we ignore it here for the sake of simplicity of our illustration and since these errors are considerably smaller than those associated with satellite rainfall products. We use the difference values between IMERG and MRMS at approximately two thousand sites located near the network confluences (Figure 1) over the whole basin to perform our evaluation (e.g., to produce the Torgegrams and covariance models).

4. Results

In Figure 2, we show the rainfall accumulations during the flood event period (September 14 through 27 September 2016) obtained from MRMS (*a*), IMERG (*b*).

The differences between IMERG and MRMS are shown in Figure 2(*c*) as a percentage of the benchmark MRMS observed rainfall as follows:

$$\text{Error} = \frac{\text{IMERG} - \text{MRMS}}{\text{MRMS}} \times 100\% \tag{1}$$

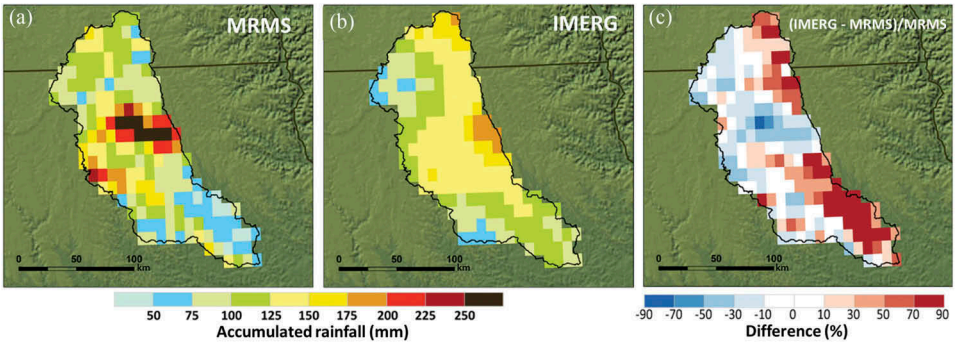

Figure 2. Rainfall accumulations during the period of (14 September 2016 through 27 September 2016) for MRMS rainfall (*a*) and IMERG rainfall (*b*). MRMS rainfall has been aggregated in space in order to be compared to IMERG. The normalized differences between the two rainfall estimates is shown as % difference in (*c*).

The comparison shows that IMERG generally over-estimated rainfall on the eastern side of the basin while missing a dense cluster of accumulation in the top half of the basin. Nevertheless, the mean areal rainfall estimates by IMERG and MRMS are almost equivalent, 123.5 and 120.5 mm respectively.

In Figure 3 we applied the accumulation method described in Quintero et al. (2016) and Cunha et al. (2015) to each rainfall product. An important feature of this figure is how the magnitude of errors in rainfall estimates accumulates downstream (i.e., the errors in lower stream orders (small streams) are much higher than the errors in high order streams). In addition, the mean areal rainfall accumulations and difference (less than 10%) are directly visible at the stream located at basin outlet. This variability in performance across scales indicates that as the basin size increases, the difference in the overall performance between the benchmark product and satellite rainfall decreases. This in turn could have implications for the performance of the hydrologic models in terms of estimated stream discharges when IMERG is used as the rainfall input (i.e., better hydrologic models' performance at larger scales; Quintero et al. 2016). Next, we investigating the semi-variance of the rainfall differences.

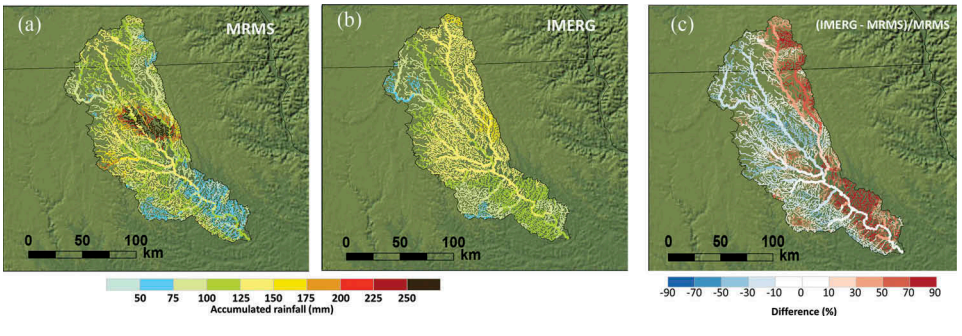

Figure 3. Rainfall accumulations during the period of (14 September 2016 through 27 September 2016) for MRMS rainfall (*a*) and IMERG rainfall (*b*). Unlike Figure 2, each product was accumulated along the stream network. The normalized differences between network based accumulations of the two products is shown as % difference in (*c*).

In case of the traditional Euclidean approach, we calculated the semi-variogram in multiple fixed directions where 0° is the North-South direction and 90° is the East-West direction (Figure 4). In Figure 4 the diameter of the semi-variance circles is proportional to the number of observations that fall in a given distance bin. It is evident that the directions with highest number of observations for longer distances are the 135° and the 0° directions because of the basin's shape and orientation. In addition, the sill was reached at distance of around 55 km for the 90° and 135° directions, and at around 30 km for the 0° and 45° directions indicating little to no autocorrelation beyond these distances.

In Figure 5(*a*), we show the Torgegram of rainfall differences obtained at the sites shown in Figure 1, where the green points are the semi-variances obtained from flow-unconnected sites, while the blue points are obtained from flow-connected sites. It is important to note that the distance used here is the stream distance, which should be generally greater than Euclidean distance due to the meandering nature of rivers and streams. This is illustrated in the Figure 5(*b*) where the distance between two flow-connected sites is represented by a solid line and the distance between two flow-unconnected sites is represented by a dashed line. The semi-variance between flow-unconnected sites is higher than the semi-variance of the connected sites at the same separation distance and extends for longer distances. The flow-unconnected semi-variogram reaches the range at around 150 km, while the flow-connected semi-varigram stops increasing at around 200 km. This difference in ranges indicates that rainfall errors among flow-connected sites are autocorrelated for longer distances compared to flow-unconnected sites. However, the flow unconnected semi-variogram experiences a large increase in semi-variance towards the end. This also occurs in the Euclidean semi-variogram in the 0° and 90° directions

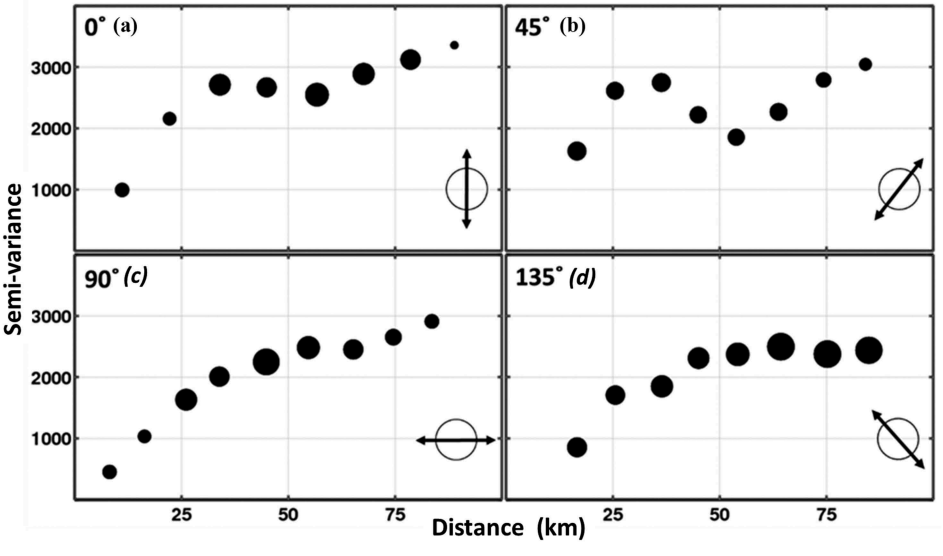

Figure 4. The directional semi-variogram obtained from the rainfall differences at the resolution of IMERG. The direction 0◦ (*a*) is the North-South while 90° (*c*) is East-West. The size of the black circles is proportional to the number of sites that are fall into a given distance bin. The circle with the arrow at the bottom right of each panel shows the variogram direction.

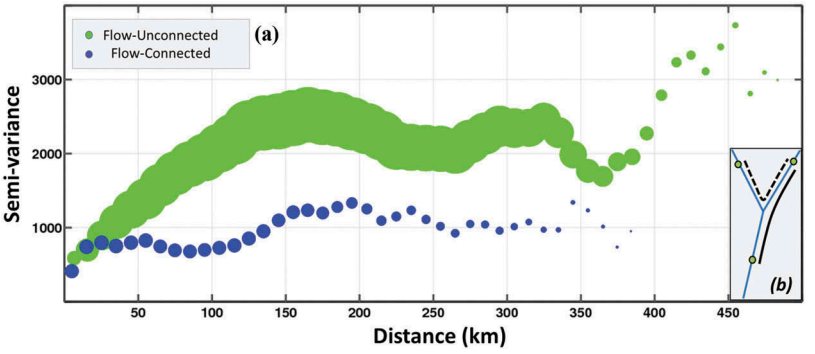

Figure 5. The Torgegram obtained using the differences calculated along the stream network (*a*). The green circles represent the flow-unconnected sites while the blue circles represent the flow-connected sites. The sizes of the circles are proportional to the number of sites that fall into a certain distance bin. The schematic on the right side (*b*), illustrates the difference between flow-connected (solid line) distances and flow-unconnected distances (dashed lines).

where the semi-variance keeps increasing without bound. In addition, it is expected that at very large distances the semi-variance for both flow-connected and flow-unconnected sites should be similar due to the absence of autocorrelation. This suggests trend contamination in the data (Zimmerman and Ver Hoef 2017).

To remove the underlying spatial trend, we begin with a visual inspection of the rainfall differences field. It suggests that for this particular storm, IMERG systematically overestimated the rainfall amounts on the eastern side of the basin while underestimating on the western side of the basin, thus causing differences in the mean value at different locations within the basin. In addition, the amount of accumulated rainfall error systematically decreases as the stream order increases. Detailed instructions on how to deal with this effect are available in Zimmerman and Ver Hoef (2017). Here, we follow their strategy and fit, by ordinary least squares, a linear model to the data using stream order, longitude, and latitude as regressors. Afterwards, we reproduce the Torgegram using the residuals of this model (Figure 6). In Figure 6, the range of the flow-unconnected sites is similar to what it was for the raw data (around 125 km) while the monotonic increase of the flow-unconnected semi-variogram has disappeared. In addition, the range of the flow-connected semi-variogram is significantly larger than that of the flow-unconnected semi-variogram (about twice as large). This linear trend-corrected Torgegram represents the hydrologically-relevant spatial dependence of satellite rainfall errors.

Our next objective is to test the predictive ability of various models of the spatial dependence. In our example, the errors are calculated and known at some 2000 locations but in some situations error prediction in river space is needed. Therefore, the next step is fitting spatial statistical models to our data. Given the nature of our variable, both tail-up and tail-down models should be important for error covariance modeling. This is because some flow-unconnected streams (especially low order streams) receive the same amount of rainfall differences due to their proximity. We compare the predictive performance of the stream network models with that of the Euclidean models.

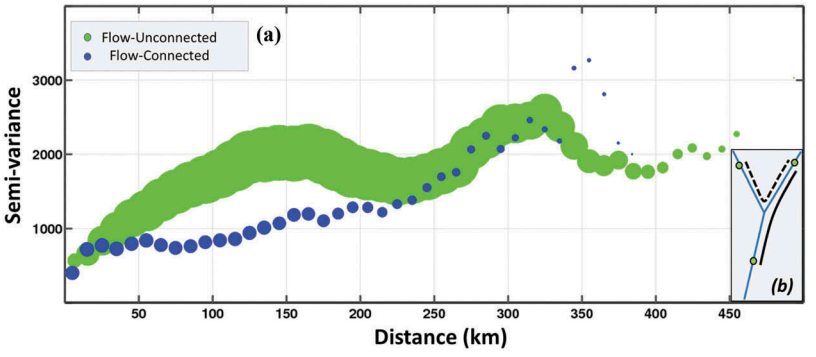

Figure 6. The Torgegram of the differences along the stream network after trend removal (*a*). The green circles represent the flow-unconnected sites while the blue circles represent the flow-connected sites. The sizes of the circles are proportional to the number of sites that fall into a certain distance bin. The schematic on the right side (*b*), illustrates the difference between flow-connected (solid line) distances and flow-unconnected distances (dashed lines).

For our example spatial linear model, we use the benchmark rainfall, upstream distance, and served (drainage) area as predictors. For the covariance of the errors, we produced linear models that leverage each of the tail-up, tail-down, and Euclidean covariance functions. In addition, we produced two mixed models, one with tail-up and tail-down, and another that included tail-up, tail-down, and Euclidean covariance models. We used spherical covariance functions for all models. We fit all models using ML to be able to compare their AIC scores (Akaike 1973). The mixed model with all covariance schemes outperformed all other models and received an AIC score of 8966. The next best model is the mixed tail-up and tail-down model, with AIC score of 9095, i.e., only slightly worse. All mixed models performed significantly better than the pure Euclidean model which resulted in 10,481 AIC score. In addition, the pure tail-up model performed worse with AIC score of 11,314; we expected this since the tail-up models allow nonzero correlation only between flow-connected sites, which is not a good representation of our variable (rainfall differences).

5. Conclusions and future work

The main goal of this study is to present a framework that could highlight the effect of basin size and stream network configuration on the performance of the satellite rainfall product IMERG Final Run in hydrological modeling applications. The process of aggregating rainfall estimates downstream in the network helps eliminate a large portion of the differences between IMERG's rainfall estimates and the benchmark product MRMS. Nevertheless, the remaining portion is correlated for much longer ranges within the stream network. Overall, stream based spatial statistical models resulted in better prediction when compared to the Euclidean distance models. However, the choice of the covariance moving average function has a strong impact on determining the model's performance. It is important to choose a moving average function that is compatible with the nature of the variable being analyzed.

This approach is also applicable to other hydrologic variables, in particular to those that result from rainfall transformation, i.e., runoff and streamflow. Specifically, we could explore the nonlinear effects of system memory, via soil moisture, on the spatial dependence of errors in flood peaks. Future work that builds on our present effort can include performing hydrologic model runs and analyzing the differences in discharges and other model variables (e.g., antecedent soil moisture) and relating them to the discrepancies in rainfall estimates.

Acknowledgments

We gratefully acknowledge the financial support from the Iowa Flood Center (IFC) towards the completion of this study. The second author was also supported by the Rose & Joseph Summers endowment.

ORCID

Mohamed ElSaadani http://orcid.org/0000-0002-0113-6175
Dale L. Zimmerman http://orcid.org/0000-0003-1212-4089

References

Akaike, H. 1973. "Information Theory and an Extension of the Maximum Likelihood Principle." In *Second International Symposium on Information Theory*, edited by B. N. Petrov and F. Caski, 267–281. Budapest: Akademiai Kiado.

Cressie, N. A. C. 1993. *Geostatistics, in Statistics for Spatial Data*. Revised ed. Hoboken, NJ: John Wiley & Sons. doi:10.1002/9781119115151.

Cunha, L. K., J. A. Smith, W. F. Krajewski, M. L. Baeck, and B. Seo. 2015. "NEXRAD NWS Polarimetric Precipitation Product Evaluation for IFloodS." *Journal of Hydrometeorology* 16: 1676–1699. doi:10.1175/JHM-D-14-0148.1.

Gourley, J. J., Y. Hong, Z. L. Flamig, J. Wang, H. Vergara, and E. N. Anagnostou. 2011. "Hydrologic Evaluation of Rainfall Estimates from Radar, Satellite, Gauge, and Combinations on Ft. Cobb Basin, Oklahoma." *Journal of Hydrometeorology* 12: 973–988. doi:10.1175/2011JHM1287.1.

Habib, E., A. T. Haile, N. Sazib, Y. Zhang, and T. Rientjes. 2014. "Effect of Bias Correction of Satellite-Rainfall Estimates on Runoff Simulations at the Source of the Upper Blue Nile." *Remote Sensing* 6: 6688–6708. doi:10.3390/rs6076688.

Hou, A. Y., R. K. Kakar, S. Neeck, A. A. Azarbarzin, C. D. Kummerow, M. Kojima, R. Oki, K. Nakamura, and T. Iguchi. 2014. "The Global Precipitation Measurement Mission." *Bulletin of the American Meteorological Society (BAMS)* 95: 701–722. doi:10.1175/BAMS-D-13-00164.1.

Huffman, G. J., D. T. Bolvin, D. Braithwaite, K. Hsu, R. Joyce, C. Kidd, E. J. Nelkin, and P. Xie, 2015. "NASA Global Precipitation Measurement (GPM) Integrated Multi-satellitE Retrievals for GPM (IMERG). Algorithm Theoretical Basis." Document, Version 4.5, 26. http://pmm.nasa.gov/sites/default/files/document_files/IMERG_ATBD_V4.5.pdf

Liu, Z. 2016. "Comparison of Integrated Multisatellite Retrievals for GPM (IMERG) and TRMM Multisatellite Precipitation Analysis (TMPA) Monthly Precipitation Products: Initial Results." *Journal of Hydrometeorology* 17: 777–790. doi:10.1175/JHM-D-15-0068.1.

Mandapaka, P. V., W. F. Krajewski, G. J. Ciach, G. Villarini, and J. A. Smith. 2009. "Estimation of Radar-Rainfall Error Spatial Correlation." *Advances in Water Resources* 32 (7): 1020–1030. doi:10.1016/j.advwatres.2008.08.014.

Peterson, E. E., and J. M. Ver Hoef. 2014. "STARS: An ArcGIS Toolset Used to Calculate the Spatial Information Needed to Fit Spatial Statistical Models to Stream Network Data." *Journal of Statistical Software* 56 (2): 1–17.

Quintero, F., W. F. Krajewski, R. Mantilla, S. Small, and B. Seo. 2016. "A Spatial–Dynamical Framework for Evaluation of Satellite Rainfall Products for Flood Prediction." *Journal of Hydrometeorology* 17: 2137–2154. doi:10.1175/JHM-D-15-0195.1.

Rodrıguez-Iturbe, I., and A. Rinaldo. 1997. *Fractal River Basins: Chance and Self-Organization*. Cambridge, UK: Cambridge University Press.

Ver Hoef, J. M., E. Peterson, and D. Theobald. 2006. "Spatial Statistical Models that Use Flow and Stream Distance." *Environmental and Ecological Statistics* 13: 449–464.

Ver Hoef, J. M., and E. E. Peterson. 2010. "A Moving Average Approach for Spatial Statistical Models of Stream Networks." *Journal of the American Statistical Association* 105: 6–18.

Vergara, H., Y. Hong, J. J. Gourley, E. N. Anagnostou, V. Maggioni, D. Stampoulis, and P. Kirstetter. 2014. "Effects of Resolution of Satellite-Based Rainfall Estimates on Hydrologic Modeling Skill at Different Scales." *Journal of Hydrometeorology* 15: 593–613. doi:10.1175/JHM-D-12-0113.1.

Villarini, G., and W. F. Krajewski. 2007. "Evaluation of the Research-Version TMPA Three-Hourly 0.25° × 0.25° Rainfall Estimates over Oklahoma." *Geophysical Research Letters* 34: L05402. doi:10.1029/2006GL029147.

Zhang, Y., D.-J. Seo, D. Kitzmiller, H. Lee, R. J. Kuligowski, D. Kim, and C. R. Kondragunta. 2013. "Comparative Strengths of SCaMPR Satellite QPEs with and without TRMM Ingest Vs. Gridded Gauge-Only Analyses." *Journal of Hydrometeorology* 14: 153–170.

Zimmerman, D., and J. M. Ver Hoef. 2017. "The Torgegram for Fluvial Variography: Characterizing Spatial Dependence on Stream Networks." *Journal of Computational and Graphical Statistics* 26 (2): 253–264.